The International Journal of Cardiovascular Imaging **19:** 157–162, 2003.

Prospective navigator gating with a dual acceptance window technique to reduce respiratory motion artifacts in 3D MR coronary angiography☆

Yiping P. Du†
Department of Radiology, Health Sciences Center, University of Colorado, Colorado, USA

Received 1 March 2002; accepted in revised form 20 November 2002

Key words: coronary artery imaging, magnetic resonance imaging, navigator echo

Abstract

A prospective navigator algorithm with a dual acceptance window (DAW) technique was developed to reduce image artifacts induced by respiratory motion without increasing imaging time. A phantom study shows that the ghost level measured by ghost-to-image ratio was reduced by 27.1% ($p < 0.005$) using the DAW technique compared to the conventional single acceptance window technique. This DAW technique can also be used to reduce imaging time while maintaining comparable ghosting level.

Introduction

Three-dimensional (3D) magnetic resonance (MR) coronary artery imaging (CAI) is subject to both cardiac and respiratory motion artifacts [1, 2]. ECG gating has been used to effectively reduce the cardiac motion artifacts. However, in 3D MR CAI techniques, the acquisition time is usually much longer than that of a breath-hold to acquire the image data. Acquiring 3D MR CAI with free-breathing requires minimal collaboration from the patients if respiratory motion artifacts can be reduced to an acceptable level. In navigated MR CAI, the diaphragm position at the right hemodome was measured to estimate the respiratory motion of the heart [3–7]. It was found that the motion of diaphragm is primarily in the superior/inferior direction [8, 9], therefore, the measurement of the diaphragm position along the superior/inferior direction can be effectively used to reduce the respiratory motion artifacts.

The respiratory motion artifacts shown in a navigated MR CAI are strongly related to the width of the acceptance window. As shown in the diminishing variance algorithm [10], motion artifacts were steadily reduced as the range of the diaphragm displacement was reduced. In another study, we have demonstrated that the views with large diaphragm displacement in retrospective navigator gating is linked to high motion artifacts in MR CAI [11]. From the motion reduction point of view, reducing the width of the acceptance window in prospective navigator is very desirable. The acceptance rate, which is the ratio between the number of views accepted and the total number of views, is decreased when the width of the acceptance window is reduced. In a typical 3D MR CAI scan with a width of the acceptance window 4 mm, the acceptance rate is in a range of 20–25% and the imaging time is in the order of 4–8 min. With the acceptance window of 4 mm in the diaphragm displacement, the width of the 'acceptance window' in the location of coronary arteries can be estimated to be in the 2–3 mm range based on the

☆The technique presented in this paper has been awarded with a US patent (US6144874) in November 2000.
†A major part of this work was conducted when the author was an employee at the Applied Science Laboratory, General Electric-Medical Systems, Milwaukee, Wisconsin, USA.

observations made by Wang et al. [8]. Compared to the typically used voxel size of $1.2 \times 1.2 \times 2\ \text{mm}^3$ and a typical diameter of coronary artery of 2–4 mm, a displacement of the coronary artery at 2–3 mm during imaging is larger than the voxel size and is about the same size of a coronary artery. This displacement of the coronary artery is large enough to cause substantial blurring and ghosting artifacts in the images.

Further reduction in the width of acceptance window would lead to a much longer imaging time. Consequently, the drift of diaphragm position [9] and gross body motion could become a dominant source of artifacts. In addition, patient discomfort would increase with a prolonged imaging time. Several techniques have been developed to reduce the respiratory motion artifacts without increasing the imaging time [12–15] based on the concept that image contrast and motion artifacts are primarily determined by the data at the central portion of *k*-space; image resolution is primarily determined by the data at the peripheral portion of *k*-space. This concept is supported by information theory that indicates that the information content in *k*-space decreases rapidly as a function of the distance from the *k*-space origin [16]. The motion-adapted gating technique [12] uses a predefined mapping function, and its modified version which uses the profile of respiratory motion measured in real-time [13], to ensure that the views with small displacement of diaphragm are placed near the center of the *k*-space; and the views with larger displacement of diaphragm are placed near the edge of the *k*-space.

Another phase reordering technique uses a respiratory profile acquired immediately prior to the acquisition of image data to map the views in an inward or outward fashion onto the *k*-space with certain mapping restrictions [14]. The phase ordering with automatic window selection technique was presented to deal with the situations in which the breathing pattern varies significantly during imaging scan [15]. While these techniques are effective, practical, and have achieved various degrees of success, the complexity of the view mapping algorithms they used has considerably increased. The effectiveness of these techniques depends on different components of their view mapping algorithms. In this paper, a simple and effective alternative approach is presented for the prospective navigator gating. In this technique, a dual acceptance window (DAW) technique is used to reduce motion artifacts without increasing the imaging time, or to reduce the imaging time with comparable motion artifacts. A phantom study is conducted to quantify the effectiveness of the DAW technique in the condition of the experiment.

Methods

Dual acceptance window

In the DAW technique, the acceptance window is divided into a central region and two peripheral regions (Figure 1a). As a result, the width of the window in the central region, as indicated as W_c in Figure 1a, is smaller than the width of the entire acceptance window, as indicated by W_p in Figure 1a. When the detected diaphragm position is located inside the central window, the phase-encoding of the subsequently acquired view is placed in the central portion of *k*-space. On the other hand, if the diaphragm position falls in one of the two peripheral acceptance windows, the subsequently acquired view is placed in the peripheral portion of the *k*-space. In the DAW technique, the views at the central part of *k*-space are filled up in an inside-out fashion; and the views at the periphery of *k*-space are filled up in an outside-in fashion (Figure 1b). When outward-growing inner region of *k*-space reaches the inward-growing peripheral region of *k*-space, the entire *k*-space is filled up, and the data acquisition is completed.

Data acquisition

3D ECG-gated gradient-echo image data were acquired with a head phantom using a head birdcage RF coil on a Signa cardiovascular MR scanner (maximum gradient amplitude = 40 mT/m, maximum slew rate = 150 T/m/s. General Electric-Medical Systems, Milwaukee, WI). The scanner table was set to an automatic rocking mode so that the phantom was moved periodically

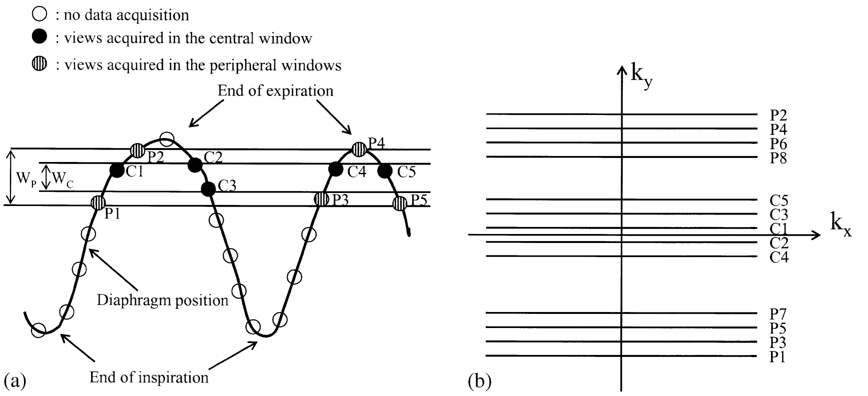

Figure 1. (a) A scheme showing the DAWs relative to the diaphragm position during free-breathing. The width of the central acceptance window is W_c; the width of the peripheral windows is W_p. Each circle represents an ECG-triggered navigator acquisition. When the position of the diaphragm was outside the acceptance windows, as shown by the open circle, no data were acquired. When the position of the diaphragm was inside the central acceptance window, shown as a solid circle, the data were acquired to fill the central region of *k*-space. When the position of the diaphragm was outside the central acceptance window but within the peripheral windows, shown as a circle filled with vertical lines, the data were acquired to fill the peripheral regions of *k*-space along the k_y direction. (b) A scheme showing the order in which the central region of *k*-space was filled for the views acquired inside the central window (i.e., C1, C2, ...). Also shown is the order in which the peripheral regions of *k*-space were filled for the views acquired in the peripheral acceptance windows (i.e., P1, P2, ...).

along the axis of the magnet to mimic the motion of the human diaphragm. The maximum displacement of the phantom was 10 mm. The profile of the motion is similar to a sinusoid function, with a frequency of approximately 0.2 Hz. The navigator echo data projections were acquired with an ECG-gated 90°–180° spin-echo navigator sequence. The column excitation of the navigator was set at the superior end of the phantom along the superior/inferior position, and it had a dimension of 20 mm × 20 mm × 100 mm. An edge detection algorithm [18] was used for accurate and robust measurement of the phantom displacement. The imaging parameters were: field of view = 340 mm × 272 mm, TE/TR/α = 1.5 ms/6.0 ms/30°, single coronal slab with matrix of 256 × 224, 12 sections, slice thickness = 3 mm, and readout bandwidth = ±31.25 kHz, and partial k_y acquisition. An electronic device was used to generate ECG signal with a heart rate of 60 beats per minute.

The DAW technique and the conventional single acceptance window (SAW) technique were used for prospective navigator gating to acquire the 3D gradient-echo images in an alternating order. In the DAW technique, the W_p was set to ±2 mm, and the W_c was set to be ±1 mm. In the SAW technique, the width of the acceptance window was set to be ±2 mm. By selecting W_p the same as the width of the acceptance window in the SAW technique, the acceptance rates, and therefore the imaging time, were approximately the same between DAW and SAW. The total imaging time to acquire a 3D image data set was about 170 s. Eleven pairs of DAW/SAW images were acquired in three different days in an effort to verify the consistency of ghost reduction using DAW.

Results

Eleven scans with the DAW technique and eleven scans with the SAW technique were performed the phantom. Motion-induced ghosting was observed in the images acquired with both techniques. The severity of ghosting was measured at the central slice in all twenty-two 3D data sets. The estimated intensity of the ghost was measured as the mean of a region-of-interest (ROI), as shown by the white square boxes in Figure 2. The intensity of the image was measured at an ROI in the liquid

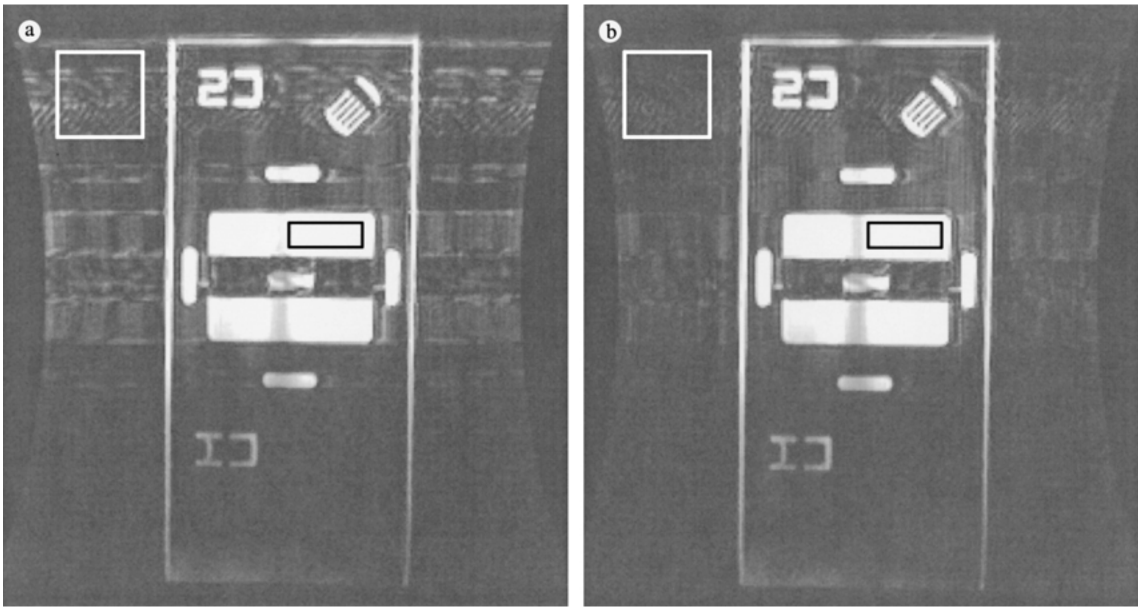

Figure 2. A typical example that of the motion-induced ghosting in the images acquired using the conventional SAW technique (a), and the DAW technique (b). In this study, the intensity of ghost is reduced by using the DAW technique. The white square boxes show the region where the intensity of ghost was measured, and the black rectangular boxes show the region where the intensity of image was measured.

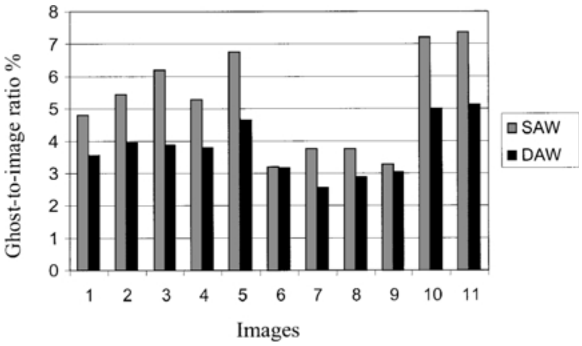

Figure 3. The comparison of the ghost-to-image ratio measurements using the DAW and SAW techniques with a rocking phantom. The ghost-to-image ratio in the eleven 3D image data sets acquired using the DAW technique were 27.1% ($p < 0.005$) lower than that in the other eleven 3D image data sets acquired using the SAW technique.

solution, as shown by the black rectangular boxes in Figure 2. The results of the ghost-to-image ratio measurement are plotted in Figure 3. In Figure 3, the image pairs 1–5, 6–9, and 10–11 were acquired in different days on the same scanner with the same protocol. The average ghost-to-image ratio with the DAW technique was 3.78% compared to 5.19% with the SAW technique. A *t*-test was applied to the measurement of ghost-to-image ratio in images acquired with DAW and SAW, as shown in Figure 3. In this experiment, a 27.1% ($p < 0.005$, τ_d test) reduction of ghost-to-image ratio was achieved using the DAW technique compared to the SAW technique.

Discussion

The ratio between the width of the central window, W_c, and the width of the peripheral windows, W_p, can readily be adjusted. This adjustment determines the tightness of the acceptance window for the central views without changing the acceptance rate. Selecting a tight central acceptance window can ensure a small deviation of the diaphragm displacement for the central views, but the number of these central views is then reduced. This leads to an increased deviation of the diaphragm position to the reference position for an increased number of peripheral views. In this study, we selected $W_c/W_p = 0.5$.

This study demonstrates that the motion artifacts can be considerably reduced by using the DAW technique with the same imaging time as SAW. The DAW technique can also be used to reduce imaging time, while maintaining a ghosting level comparable to SAW. In that approach, we can properly increase the width of the peripheral window such that the increased motion artifacts resulting from the increased width of the peripheral window are approximately compensated for by the reduced motion artifacts using DAW.

In the implementation of DAW, the first view acquired at the small window, S1, and the first view acquired at the large window, L1, should be placed at opposite sides of the k_y-direction. For example, if S1 is placed at $k_y > 0$ and L1 should then be placed at $k_y < 0$, as shown in Figure 1b. With this view ordering, the *k*-space will be entirely filled up when a total of N_y views have been accepted; where N_y is the number of sampling lines along the phase-encoding direction. If S1 and L1 are placed at the same side along k_y, one view at k_y will be blank; and the other view along k_y will be sampled twice when an odd number of views are acquired in the small window and an odd number of views are acquired in the large window.

The phantom images were acquired in different days on the same scanner with the same protocol. The results of the DAW technique show a consistent ghost reduction in each pair of the images compared to the SAW technique (see Figure 3). Figure 3 also show that the highest ghost-to-image ratio acquired with DAW is below the lowest ghost-to-image ratio acquired with SAW in each group of image pairs acquired in the same day (i.e., image pairs 1–5, 6–9 and 10–11). The reason for the higher variation of ghost-to-image ratio observed in different days (see Figure 3) is not clear, although it is suspected that the difference in the placement of the phantom in different days may contribute in certain degree.

In theory, increasing the number of divisions in the acceptance window could further improve the distribution of acquired views in *k*-space based on the deviation of diaphragm position to a 'reference' position. In an ideal condition, the 'k_y distance' from a view to be placed to the central view (i.e., $k_y = 0$) should be a monotonic function of the diaphragm displacement relative to the 'reference' position. In other words, the views acquired with smaller diaphragm displacement should be placed at a *k*-space location closer to $k_y = 0$. Because we do not have prior knowledge about the diaphragm displacement of the upcoming views, this ideal condition cannot be exactly satisfied. The hybrid ordering of phase-encoding (HOPE) algorithm [17] is an approximation of this ideal case. The HOPE algorithm maps the most frequent diaphragm positions to the central regions of *k*-space and uses the probability distribution to map the remaining positions. If more than two divisions of the acceptance window are selected, a dynamic algorithm, such as HOPE, would be needed to fill in *k*-space without discarding the 'good' views that are acquired within the acceptance windows. With two divisions, the scheme to fill up the *k*-space as proposed in this paper is rather straightforward and can be easily implemented.

Summary

In the proposed DAW technique of prospective navigator gating, the views acquired with smaller diaphragm displacement relative to the reference position were placed at the central portion of the *k*-space; the views acquired with larger diaphragm displacement were placed at the peripheral region of the *k*-space. This study conducted with a phantom shows that the DAW technique can reduce the intensity of motion-induced ghosting by 27.1% ($p < 0.005$) without increasing imaging time. This DAW technique can also be used to reduce imaging time by increasing the width of the acceptance window while maintaining ghosting level comparable to SAW.

Acknowledgement

The author thanks Dr D.A. Bluemke at Johns Hopkins Hospital and Drs T.K.F. Foo, M. Saranathan at GE-Medical Systems for their helpful discussions.

References

1. Li D, Paschal CB, Haacke EM, Adler LP. Coronary arteries: three-dimensional MR imaging with fat saturation and magnetization transfer contrast. Radiology 1993; 187: 401–406.
2. Hofman MBM, Paschal CB, Li D, Haacke EM, van Rossum AC, Sprenger M. MRI of coronary arteries: 2D breath-hold vs 3D respiratory-gated acquisition. J Comput Assist Tomography 1995; 19: 56–62.
3. Liu YL, Riederer SJ, Rossman PJ, Grimm RC, Debbins JP, Ehman RL. A monitoring, feedback, and triggering system for reproducible breath-hold MR imaging. Magn Reson Med 1993; 30: 507–511.
4. Wang Y, Grimm RC, Rossman PJ, Debbins JP, Riederer SJ, Ehman RL. 3D coronary MR angiography in multiple breath-holds using a respiratory feedback monitor. Magn Reson Med 1995; 34: 11–16.
5. Wang Y, Rossman PJ, Grimm RC, Riederer SJ, Ehman RL. Navigator-echo-based real-time respiratory gating and triggering for reduction of respiratory effects in three-dimensional coronary MR angiography. Radiology 1996; 198: 55–60.
6. Li D, Kaushikkar S, Haacke EM, et al. Coronary arteries: three-dimensional MR imaging with retrospective respiratory gating. Radiology 1996; 201: 857–863.
7. Danias PG, McConnell MV, Khasgiwala VC, Chung ML, Edelman RR, Manning WJ. Prospective navigator correction of image position for coronary MR angiography. Radiology 1997; 203: 733–736.
8. Wang Y, Riederer SJ, Ehman RL. Respiratory motion of the heart: kinematics and the implications for the spatial resolution in coronary imaging. Magn Reson Med 1995; 33: 713–719.
9. Taylor AM, Jhooti P, Wiesmann F, Keegan J, Firmin DN, Pennell DJ. MR navigator-echo monitoring of temporal changes in diaphragm position: implications for MR coronary angiography. J Magn Reson Imaging 1997; 7: 629–636.
10. Sachs TS, Meyer CH, Irarrazabal P, Hu BS, Nishimura DG, Macovski A. The diminishing variance algorithm for real-time reduction of motion artifacts in MRI. Magn Reson Med 1995; 34: 412–422.
11. Du YP, McVeigh ER, Bluemke DA, Silber HA, Foo TKF. A comparison of prospective and retrospective respiratory navigator gating in 3D MR coronary angiography. Int J Card Imaging 2001; 17: 287–294.
12. Weiger M, Bornert P, Proksa R, Schaffter T, Haase A. Motion-adapted gating based on *k*-space weighting for reduction of respiratory motion artifacts. Magn Reson Med 1997; 38: 322–333.
13. Sinkus R, Bornert P. Motion pattern adapted real-time respiratory gating. Magn Reson Med 2000; 41: 148–155.
14. Jhooti P, Keegan J, Gatehouse PD, et al. 3D coronary artery imaging with phase reordering for improved scan efficiency. Magn Reson Med 1999; 41: 555–562.
15. Jhooti P, Gatehouse PD, Keegan J, Bunce NH, Taylor AM, Firmin DN. Phase ordering with automatic window selection (PAWS): a novel motion-resistant technique for 3D coronary imaging. Magn Reson Med 2000; 43: 470–480.
16. Fuderer M. The information content of MR images. IEEE Trans Med Imaging 1988; 7: 368–380.
17. Jhooti P, Wiesmann F, Taylor AM, et al. Hybrid ordered phase encoding (HOPE): an improved approach for respiratory artifact reduction. J Magn Reson Imaging 1998; 8: 968–980.
18. Du YP, Saranathan M, Foo TKF. A computationally efficient algorithm for accurate detection of diaphragm displacement in navigated 3D coronary MR angiography. Proceedings of the Eighth Scientific Meeting of ISMRM. Denver, 2000; 1624.

Address for correspondence: Yiping P. Du, Department of Radiology, Health Sciences Center, University of Colorado, 4200 E. 9th Avenue, Box C-278 Denver, CO 80262, USA
Tel.: +303-315-8468; Fax: +303-315-8993
E-mail: yiping.du@uchsc.edu